

Numerical Evaluation of Punching Shear Capacity Between Bonded and Unbonded Post-tensioned Slab Using Inverted-U Shape Reinforcement



Milad Khatib and Zaher Abou Saleh

Abstract The Both bonded and unbonded prestressing tendons may be used to reinforce post-tensioned (PT) concrete members. The binding state of tendons may have an impact on how well different types of PT concrete elements function in flexural and shear loads. Inverted-U shape reinforcement was used experimentally to enhance the behavior of different structural elements. The obtained results confirmed the proposed model's accuracy for both PT slabs and beams (bonded, and unbonded). This study's major goal is to compare numerically PT concrete slabs provided with inverted-U shape reinforcement with the two different tendon systems and evaluate their performances due to applying punching shear load. To do this, the PT slab that has already been tested is reexamined numerically. By using, a nonlinear finite element, the results were carried out utilizing visualization tools. For a better study of the behavior of bonded and unbonded PT slabs, the obtained numerical results, and the previous experimental one are compared. Good correlations are shown.

Keywords Bonded Tendons · Unbonded Tendons · Post-tension Slab · Inverted-U Shape Reinforcement · Nonlinear Finite Element

1 Introduction

Today, many structures require prestressed concrete in order to use the minimum concrete slab thickness and, reduce of both cracks and deflection. Pretensioned, unbonded, and bonded PT prestressed concrete are the three types of prestressed concrete construction. The study of structural mechanisms in PT concrete members

M. Khatib (✉)
Research Supervisor Civil Engineering, ISSEA-Cnam, Beirut, Lebanon
e-mail: milad.khatib@isae.edu.lb

Z. A. Saleh
Co-Founder & CEO LTC, Jiyeh, Lebanon

© The Author(s) 2023
G. Feng (ed.), *Proceedings of the 9th International Conference on Civil Engineering*,
Lecture Notes in Civil Engineering 327,
https://doi.org/10.1007/978-981-99-2532-2_50

still requires to be considerably improved in several aspects, like shear-flexure interactions in PT slab. Moreover, investigations comparing the differences between the slabs, bonded and unbonded, were rarely discussed, and published. The behaviors of PT concrete beams and slabs one-way with various tendon-bonding parameters have only been compared in a few studies.

1.1 Review

Freyssinet had develop the first application of post-tensioning for the construction of a Normandy marine port in France. This technique was established in the United States in the 1950s [1].

The guidelines for assessing the vibration serviceability of thin post-tensioned concrete floors have shown to be inaccurate. Some researchers validated a set of empirically rules for performing out such analysis. It has been shown that the elastic modulus of essential columns contributes significantly to the total elastic modulus of the floor, and that they should not be treated as pin supports that allow unrestricted rotation. The usage of bar finite elements to replicate the columns worked well [2].

A potentially weak PT beam was kept after the entire dismantling of a prestressed concrete bridge in southern France for non-destructive testing (NDT), then reviewed all the outcomes of four alternative approaches [3]. By focusing on ambiguous zones to get accurate local measurements or by enhancing measurement reliability, the adoption of a different approach should give a more appropriate response while removing certain ambiguities. The issues that these methods have not fully addressed are then identified. The collection of demands that these strategies have thus far failed to satisfy comes as the final phase.

Later, five internal connections were tested experimentally. Each one was consisted of two PT beams (top-and-seat-angle wide flange) connected to a column. These connections were seismically loaded on steel moment resistant frames. The number of PT strands were considered as the studied factors, and the initial post-tensioning force. The connections were fabricated, in such a way, that the energy was dissipated in the angles; while the other structural parts remain elastic. The obtained results showed that PT connectors have significant cyclic strength and ductility. The preliminary elastic stiffness is equivalent to that of a welded connection, and the connection has almost no structural damage after extreme inelastic drifted cycles [4].

A numerical model was suggested to estimate the response of unbonded PT beams. The effects of monotonic and repetitive loads are both examined. The model's uniqueness may be seen in the estimation of prestressed concrete serviceability following cracking, which is based on a non-linear macro finite element model. It was distinguished by its homogenous average inertia. A second novelty was the estimation of total elongation for the unbonded tendons at all stress phases: cracking, serviceability, and ultimate. The results demonstrate that the model predicts the bending stiffness of the beam during loading cycles and the stable remaining deflection after

unloading related to crack development. Both of bearing capacity and deflection at failure estimations are also quite precise [5].

A clear evaluation was conducted between members with the two distinct tendon systems and examine their structural behavior in detail. Actually identified PT beams, one-way slabs, and slab-column connections were reevaluated, and extensive nonlinear finite element calculations were undertaken utilizing new modelling approaches. A set of test results demonstrates that the established model was trustworthy for both bonded and unbonded PT parts. The findings of the earlier experimental and present numerical investigations are utilized for better examining the behavior of bonded and unbonded PT components [6].

Punching shear reinforcement is a practical method for enhancing the strength and deformation resistance of flat slabs. Such reinforcement have been produced in many forms in the past. With “Inverted-U Shaped Reinforcement,” an unbonded PT slab, was exposed numerically to punching loads, and examined [7]. The outcomes were compared with those from an earlier experimental study. There was a good relation between all the obtained results (numerically and experimentally).

An experimental PT beams provided with bonded and unbonded tendons were studied [8]. These tendons were referred as “mixed tendons”. A numerical evaluation for the obtained results were achieved using finite element model. The proposed numerical technique reported was proven to accurately estimate ultimate flexural strength, mode of failure, and tendon stress within 5%. The final displacement was predicted quite well (around 15%) for the mixed tendons.

PT concrete beams prevent shear via a variety of mechanisms. Special shear reinforcement can be utilized to improve the shear capacity of such beams. A conducted experiment studied the effect of inverted-U shape reinforcement on the shear strength of bonded PT concrete beams. The results were compared to another type of bonded PT concrete beams, which provided with conventional type of reinforcement against shear (closed stirrups). The results indicate a 13% improvement in shearing strength. There are important correspondences between projected and actual experimental outcomes [9].

Four unbonded PT beams were tested. During the tests, several data were collected. The obtained results were compared to the currently used methods in Russia. Tests and calculation results demonstrate that Russian analytical techniques are underestimated for the unbonded PT beams design [10].

In order to enhance the concrete shear strength of PT beams utilizing various shear reinforcing methods, several tests and computational analysis were carried out. An investigation for the benefit of inverted-U shaped reinforcement in bonded PT beams, experimentally, was conducted. Recently, numerical investigation was carried to explore the impact of these reinforcement on the shear behavior of two types bonded PT beams [11]. The numerical outcomes showed that the ACI 318–14’s restriction on the nominal shear reinforcement for bonded pre-stressed concrete beams was overly cautious [12].

2 Objectives of the Investigation

The aim of this study is to apply numerically a punching load on two types of bonded PT slabs, the first one provided with inverted-U shaped reinforcement, while the other provided with stud reinforcement, and then analyze their behaviors in terms of load deflection relationship as well as average shear strength around the critical shear zone. A previous numerical unbonded PT slab subjected to punching load was achieved.

Unbonded tendons provide unique structural benefits rather than bonded tendons, the post-flexural catenary capacity. It is nearly hard to fail an unbonded tendon under tension according to applied force. This component provides apparent benefits under extreme loading or in reducing punching shear failure. Tests have revealed that slabs with unbonded tendons contain catenary capacities three to four times the requirement at factored load [13].

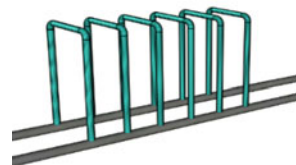
Since the bonded circumstances seem to be the worst situation for the unbonded ones, then a finite element program “ABAQUS” is applied to provide numerical conclusions for this situation, and compare it with the unbonded one [14]. Those findings were examined with those previously obtained through an experimental evaluation of the punching shear strength utilizing unbonded PT concrete slabs with “Inverted-U Shaped Reinforcement” and the ACI specifications for punching shear strength.

3 Numerical Unbonded Investigation

A numerical research, using finite element analysis FEA, was suggested [7]. Set of inverted-U shaped reinforcement (Fig. 1) were inserted in the punching shear zone of unbonded PT concrete slab (PT-A). The slab structure is vertically symmetric about an axis at centerline, and had dimensions $1.8 \times 1.8 \times 0.01$ m. (Fig. 2).

These dimensions were set to yield at a nominal punched shear stress (approximately 25 tons) by using ACI formula for stud shape ($0.66 \sqrt{f'_c}$ at a distance $d/2$ from the column face). An upward statically force was exerted across a central surface (10×10 cm). Six tendons were placed in each direction. The PT forces (146.5 kN) were supplied in a separate phase. The flat concrete slab was prevented from sliding by four fixed supports, which situated 90 cm apart from center and extended 45 cm on

Fig. 1 Hairpin shaped reinforcements



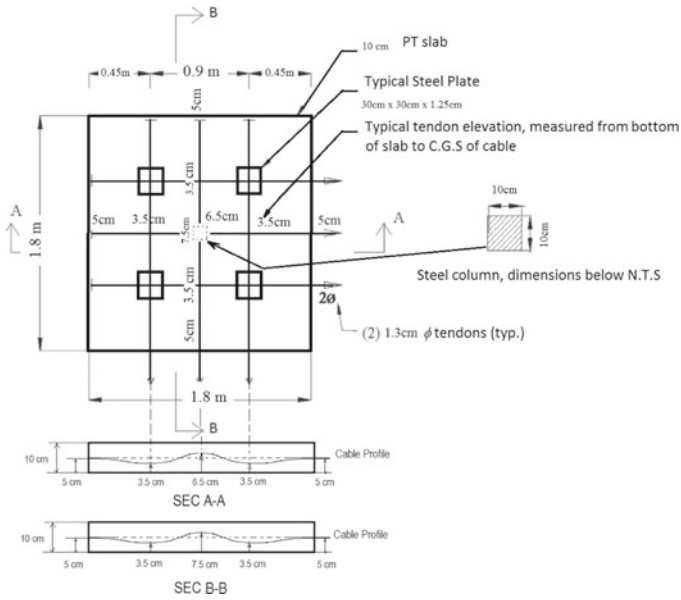


Fig. 2 Unbonded PT Tendon layout in PT slab [7]

every edge. Longitudinal and transverse reinforcing steel bars were placed under the four steel supports (Fig. 3).

The purpose of this numerical research, using ABAQUS, was to analyze the behavior of unbonded PT flat slab provided with inverted-U shaped reinforcement in the center area, and subjected to punching shear force as indicated in Fig. 4. The

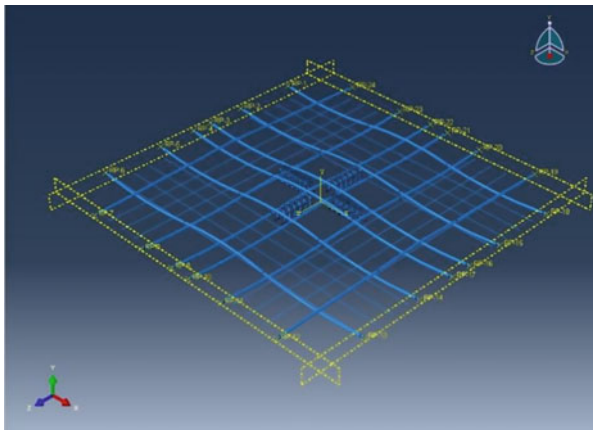


Fig. 3 PT Tendons and Reinforcement Layout

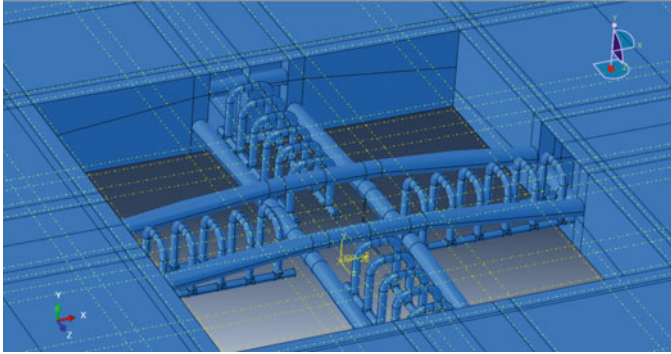


Fig. 4 Unbonded PT Slabs Reinforcement Provide with Inverted-U Shaped Reinforcement (PTU-A)

Fig. 5 Stud Reinforcement



investigation was also undertaken on another unbonded PT concrete slab (PT-B) provided with stud reinforcement (Fig. 5) to evaluate, and compare the results.

ABAQUS is a useful program for FEA, initially introduced in 1978. The study of a structural system is accomplished through three processes. Firstly, specify the FE model and external conditions to be applied to it (Pre-processing). Then, this FE model will be simulated (Analysis solver or Simulation). Finally, analyze the generated data (Post-processing). By utilizing the visualization module, numerous outcomes can be examined by showing the results, such as contour lines, deformed shapes, and X–Y plots.

The compressive strength of utilized concrete was 30 MPa; the prestressing strands were 12.5 mm diameter complying to ASTM standard A421, with a required ultimate strength of 1860 MPa. Bars of 10 mm were utilized for modelling of both 6 hairpins reinforcement (PT-A) and 6 studs (PT-B) for each direction. The shear reinforcement of both specimens have such a yielding strength of 420 MPa.

4 Numerical Unbonded Investigation

A smoothly grading crack forms when the load increases on the unbonded slab with inverted-U shaped reinforcement (PTU-A). The sequential cracks development signifies that major, flexural and diagonal ones, developed at more than yielding of steel bars. At a compression force of 290 kN, the slab collapsed because the cracks expanded towards top, with corresponding deflection equals to 19.30 mm (Fig. 6). The slab collapsed in flexural mode prior to punching shear.

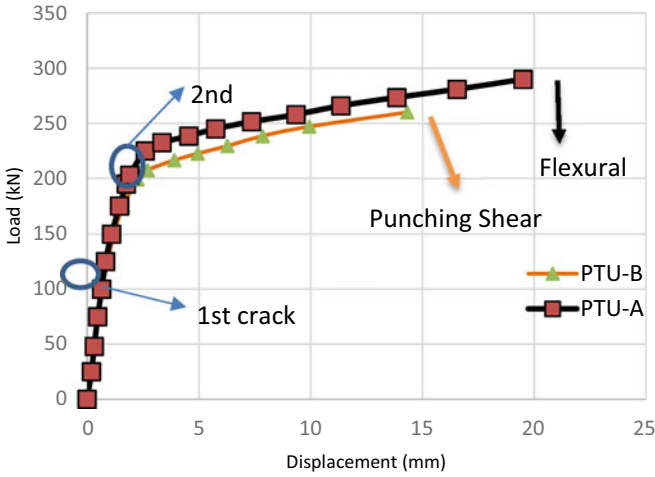


Fig. 6 The Load–Deflection Curves for PTU-A & PTU-B

Regarding the second unbonded slab type with stud reinforcement (PTU-B), it was found that the fractures appeared in a sudden manner. With increased load, further shear fractures formed. As the observed load reached to 260 kN, the top of the slab cracked with maximum deflection corresponds to 14.32 mm (Fig. 6). This slab collapsed in shear mode.

All the numerical results for the two types of unbonded slabs (PTU-A) and (PTU-B) are reported in Table 1.

It was clear that the load capacity for the (PTU-A) was increased about 10.34% than the (PTU-B). In addition, (PTU-A) resisted the punching shear stresses more than (PTU-B) by 10.50%. However, the (PTU-A) failed in flexural mode, while the (PTU-B) failed in shear mode.

The obtained results for PTU-A were improved than PTU-B by 10.34% concerning failure load, and 10.50% regarding nominal shear stresses.

Table 1 Numerical results for “Unbonded” PT Slabs

| Specimen designation | Reinforcement type | Failure loads (kN) | Deflection (mm) | Nominal shear stress (MPa) | Failure type |
|----------------------|--------------------|--------------------|-----------------|----------------------------|----------------|
| PTU-A | Inverted-U | 290 | 19.30 | $4.76 = 0.87 \sqrt{f'c}$ | Flexural |
| PTU-B | Stud | 260 | 14.32 | $4.26 = 0.78 \sqrt{f'c}$ | Punching Shear |
| % difference | | 10.34% | 25.80% | 10.50% | |

5 Numerical Bonded Investigation

The greater part of PT tendons being used in unbonded PT slabs. In the United States only, and by the mid of 2006, more than 50% of the residential structures, use the PT concrete. Moreover, it was expected that over 375,000 residences will be built using PT method annually. Furthermore, slabs with bonded tendons are widely utilized in other regions of the world [15]. By the end of 2012, it was estimated that more than 2.5 billion ft² with unbonded PT slabs in use in the United States [16].

The FEA for bonded PT concrete slab provided with inverted-U shaped reinforcement (PTB-A) is proposed and developed, which will include material parameters, element types, and analysis processes. The same development will be followed for the bonded PT concrete slab provided with stud reinforcement (PTB-B).

5.1 Concrete and Steel Material Modeling

All the utilized materials characteristics in the model are similar to that in the prior numerical model. A mix of 3D solid and truss components are used to model the simulated structures.

Concrete is modelled by utilizing the installed “damaged plasticity model” in ABAQUS [14]. The theory of “Concrete Damaged Plasticity” (CDP) was distinguished in 1989 [17], and later confirmed in 1998 [18]. By using it, the three-dimensional stress–strain controlling equations are derived from the uniaxial stress–strain relationship of concrete. The uniaxial stress–strain compression relationship is computed based on an available empirical approach [19]. Recently, many investigations have shown that the damage plasticity model provides an accurate technique for simulating concrete behaviour in both of the tension and the compression [20–22]. The tensile relationship is considered straight until cracking, and, for post-cracking behavior, is modelled using tension stiffening. The tension stiffening effect is considered minor enough that the stress following cracking gradually falls to a minimum value at about nearly twice the cracking strain. This concept was demonstrated to be appropriate for PT slab [23]. Just for simplicity, the nonlinear stress–strain curves are divided into piecewise linear parts as illustrated in (Fig. 7).

For mild steel, the behavior is perfectly elasto-plastic. However, the tendons had a nonlinear behavior one. For the PT tendons, the nonlinear stress–strain relationship is computed based on empirical approach [24] for seven wire strands (Grade 270).

5.2 Elements

Two types of ABAQUS elements are utilized in the constructed models. The rebar reinforcement are modelled by applying a sequence of linear truss elements (T3D2:

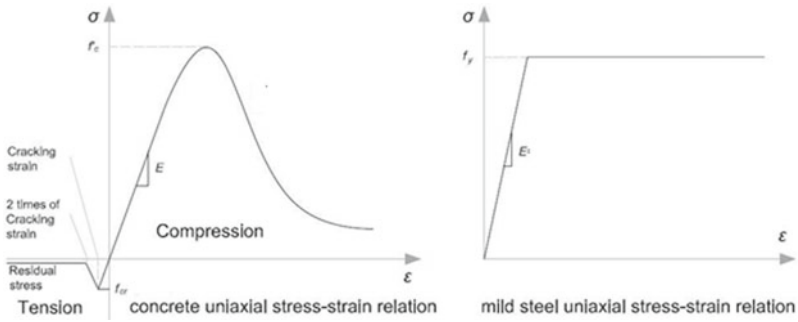


Fig. 7 Uniaxial Stress–Strain Models for FEM

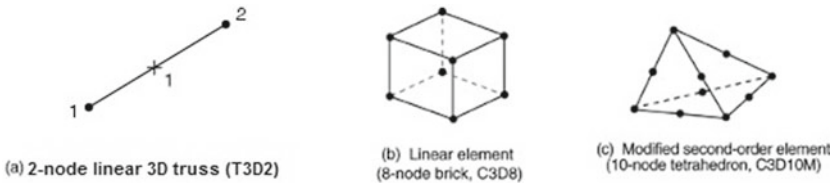


Fig. 8 Elements Abaqus

three-dimensional, and two nodes, Fig. 8a). This element can be utilized to model the tendons. However, it does not have external surface, so we cannot make a surface cohesion with the concrete.

Then, the solid element (C3D8R: three-dimensional, eight nodes, and linear with reduced integration, Fig. 8b) is the solution for this problem. In addition, this element is used to model the concrete.

The two reinforcement types against shear (inverted-U and stud) are modelled using the element (C3D10M: three-dimensional, and ten nodes modified, Fig. 8c).

Modeling Interaction Between Reinforcement and Concrete. All used rebars, inverted-U and stud reinforcement are considered as fully bonded. The embedding approach is used in the modelling to fulfill the perfect bond requirement. The bonded aspect of prestressing tendons, and large tendons sliding are modelled using the contact formulation [23].

The bonding conditions mechanism may be reproduced by utilizing a contact formulation between tendons and concrete (surface-to-surface contact, Fig. 9).

The tangential behavior of the surface contact is designed to be frictionless for the PT period, enabling the tendon to glide easily. To replicate the grouting process, the modeling approach for the tangential contact concept is changed from "frictionless" to "rough". Mesh slab is shown in Fig. 10, while fixed support conditions and applied loads are shown in Fig. 11.

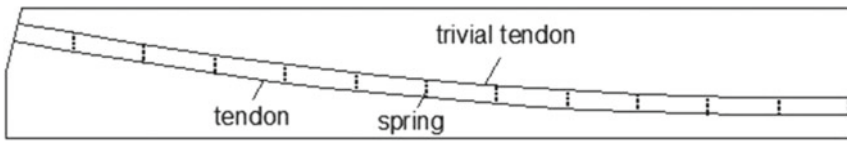


Fig. 9 Modeling Details for Unbonded PT Tendons [23]

Fig. 10 Meshed PT Slab

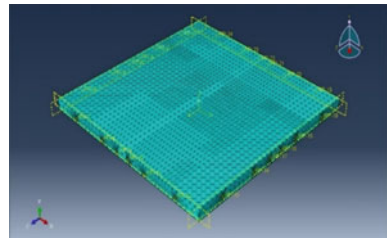
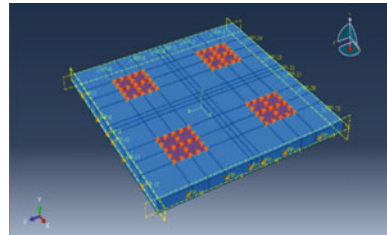


Fig.11 Boundary Conditions PT Loaded Slab



6 Numerical Bonded Results

All the obtained results for modeled bonded slabs provided with both of inverted-U shaped reinforcement (PTB-A), and stud reinforcement will be discussed as follows:

6.1 Bonded PT Slabs with Inverted-U Shaped Reinforcement: PTB-A

As the load increases, a uniform scaled fracture appears on the load–deflection curve (Fig. 12) and the distorted colored outline contour plots (Figs. 13(a), and 13(b)).

However, at mid-span, a significant deflection occurred. The crack developments indicate that considerable, flexural and diagonal fractures occur further than the yielding value of reinforcement rebars. The slab collapsed in flexural mode with an applied load equal to 270 kN with corresponding deflection of 8.43 mm.

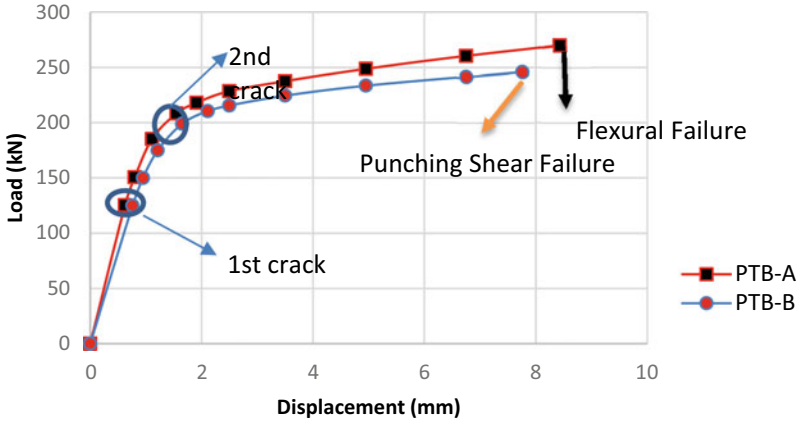


Fig. 12 The Load–Deflection Curves for PTB-A & PTB-B

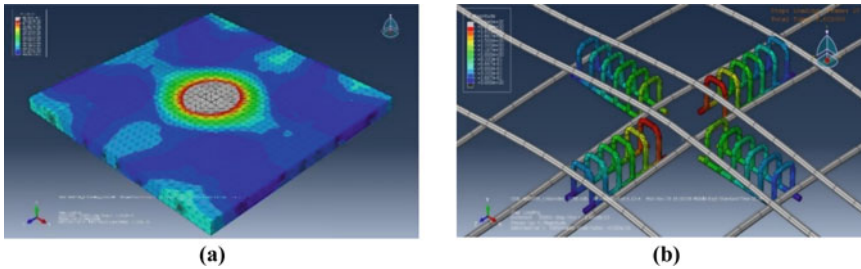


Fig. 13 a Directional Deformation for Bonded PTB-A. b Directional Deformation for Bonded PTB-

6.2 Bonded PT Slabs with Stud Shaped Reinforcement: PTB-B

Based on the obtained numerical results (Fig. 12) and the distorted colored contour plots (Fig. 14(a) and 14(b)), it appears that the fractures occurred suddenly. The shear fractures occurred as the strain increased. The slab model collapsed in shear mode with a deflection of 7.76 mm at 246 kN, the highest reached load.

In bonded cases, PTB-A resists punching load greater than PTB-B by 10.72%, while sustains more nominal shear stresses by 32.50%.

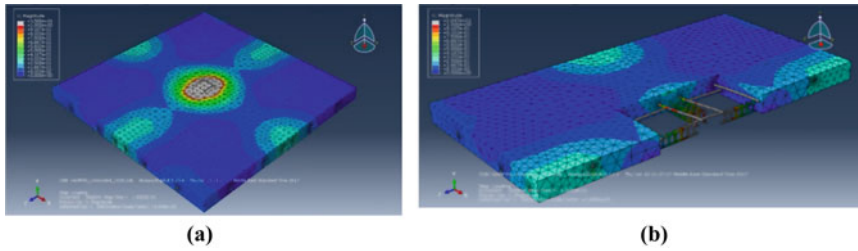


Fig. 14 a Directional Deformation for Bonded PTB-B. b Directional Deformation for Bonded PTB-B

7 Comparison Between Numerical Results

The displayed load deformation curves in Fig. 13 are based on the obtained numerical findings from for both of the bonded models, PTB-A and PTB-B. The positive influence of inverted-U shaped reinforcement on the deflection can be seen compared to stud reinforcement.

Table 2 summarize the results of nominal shear stresses at the boundary of punching shear on the top surface of the slab for bonded PT slabs provided with both of “inverted-U shaped” and “stud”. The load capacity of (PTB-A) was clearly increased by 8.88% over (PTB-B). Furthermore, the (PTU-A) resist the punching shear stresses by 10.34% more than (PTU-B). The (PTU-A) nevertheless failed in flexural mode, whilst the (PTU-B) failed in shear mode.

All the obtained results for the unbonded and the bonded slabs are summarized in Table 3. The load capacity for PTU-A was decreased by 6.90% comparing to PTB-A, and the nominal shear stress was reduced by 8.20% (Fig. 15). While, for the slab PTU-B, there is a reduction of both the capacity load about 5.38% from PTB-B, and 30.75% for the nominal shear stresses (Fig. 16).

Table 2 Numerical results for “Bonded” PT Slabs

| Specimen Designation | Reinforcement Type | Failure Loads (kN) | Deflection (mm) | Nominal Shear Stress (MPa) | Failure Type |
|----------------------|--------------------|--------------------|-----------------|----------------------------|----------------|
| PTB-A | Inverted-U | 270 | 8.43 | $4.37 = 0.79 \sqrt{f'c}$ | Flexural |
| PTB-B | Stud | 246 | 7.76 | $2.95 = 0.54 \sqrt{f'c}$ | Punching Shear |
| % difference | | 8.88% | 7.94% | 32.50% | |

Table 3 Numerical Comparison between “Unbonded” and “Bonded” PT Slabs with ACI provisions

| Specimen Designation | Reinforcement Type | Numerical Results | | | ACI Equation |
|----------------------|--------------------|--------------------|-----------------|----------------------------|----------------------------|
| | | Failure Loads (KN) | Deflection (mm) | Nominal Shear Stress (MPa) | Nominal Shear Stress (MPa) |
| PTU-A | Inverted-U | 290 | 19.30 | $4.76 = 0.87 \sqrt{f'c}$ | Not Applicable |
| PTB-A | | 270 | 8.43 | $4.37 = 0.79 \sqrt{f'c}$ | |
| % difference | | 6.90% | 56.32% | 8.2% | |
| PTU-B | Stud | 260 | 14.32 | $4.26 = 0.78 \sqrt{f'c}$ | $0.66 \sqrt{f'c} = 3.614$ |
| PTB-B | | 246 | 7.76 | $2.95 = 0.54 \sqrt{f'c}$ | |
| % difference | | 5.38% | 45.81% | 30.75% | |

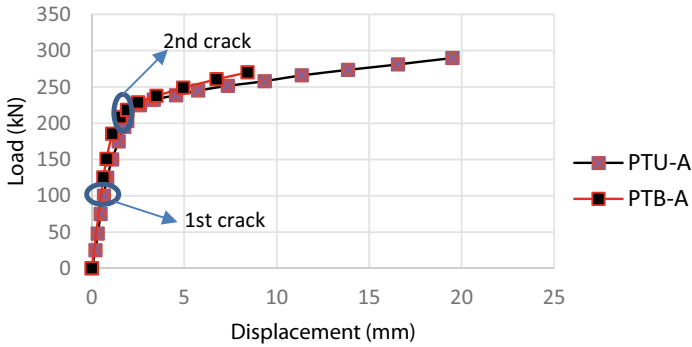


Fig. 15 The Load–Deflection Curves for PTU-A & PTB-A

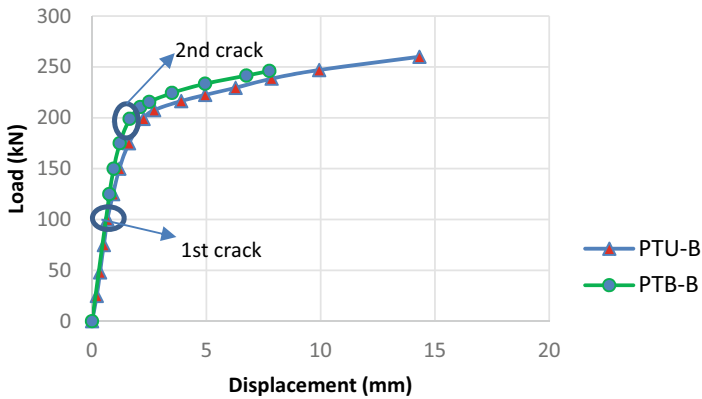


Fig. 16 The Load–Deflection Curves for Bonded PTB-B & PTU-B

8 Discussions and Conclusions

Despite the absence of studies on the real stress behavior of bonded slabs, and their construction methods outside the US, it appears reasonable that ACI 318 should impose a same quantity of reinforcement for bonded PT slabs, as is needed in unbonded PT slabs.

The slab provided with inverted-U shaped reinforcement resist punching load more than the slab provided with stud reinforcement, in both cases of unbonded (10.34%) and bonded (8.88%).

Although, the slab provided with inverted-U shaped reinforcement has nominal shear stress higher than the slab provided with stud reinforcement, in both cases of unbonded (10.50%) and bonded (32.50%). These improvements in the studied values were due to confinement of the concrete.

Finally, it is predicted that the increased quantity of bonded reinforcement necessary to meet the parameters specified herein would be minor, posing no major economic penalty for the use of bonded tendons in PT slabs while providing a large performance gain.

9 Further Research

Checking concrete slabs with bonded tendons will show that this proposal is conservative; however, until such testing is available, these proposals should be preceded to confirm the same performance level, and safety in bonded slabs as has been indicated by experiments and performance in slabs provided with unbonded tendons.

References

1. Xercavins P, Demarthe D, Shushkewich K (2010) Eugene Freyssinet – His Incredible Journey to Invent and Revolutionize Prestressed Concrete Construction. 3rd fib International Congress
2. Pavic A, Reynolds P, Waldron P, Bennett K (2001) Dynamic modelling of post-tensioned concrete floors using finite element analysis. *Finite Elem Anal Des* 37(4):305–323. [https://doi.org/10.1016/S0168-874X\(00\)00045-7](https://doi.org/10.1016/S0168-874X(00)00045-7)
3. Dérobert X, Aubagnac C, Abraham O (2002) Comparison of NDT techniques on a PT beam before its autopsy. *NDT E Int* 35(8):541–548. [https://doi.org/10.1016/S0963-8695\(02\)00027-0](https://doi.org/10.1016/S0963-8695(02)00027-0)
4. Garlock MM, Ricles JM, Sause R (2003) Experimental studies on full-scale post-tensioned seismic-resistant steel moment connections. Book *Stessa*, 1st edn ISBN:9780203738290
5. Vu NA, Castel A, François R (2010) Response of PT concrete beams with unbonded tendons including serviceability and ultimate state. *Eng Struct* 32(2):556–569. <https://doi.org/10.1016/j.engstruct.2009.11.001>
6. Kang TH-K, Huang Y, Shin M, Lee JD, Cho AS (2015) Experimental and numerical assessment of bonded and unbonded post-tensioned concrete members. *ACI Struct J* 112(6):735–748. <https://doi.org/10.14359/51688194>

7. Khatib M, Abou Saleh Z, Baalbaki O, Temsah Z (2018) Numerical punching shear analysis of unbonded post-tensioned slabs with inverted-u shaped. *KSCE J Civil Eng* 22:4490–4499. <https://doi.org/10.1007/s12205-018-1505-5>
8. Brenkus N, Tatar J, Hamilton H, Consolazio G (2019) Simplified finite element modeling of PT concrete members with mixed bonded and unbonded tendons. *Eng Struct* 179:387–397
9. Khatib M, Abou Saleh Z (2020) Enhancement of shear strength of bonded post-tensioned beams using inverted-U shaped reinforcements. *Case Stud Construct Mater* 13. <https://doi.org/10.1016/j.cscm.2020.e00370>
10. Gavrilenko A, Barkaya T (2021) Experimental and theoretical study of post-tensioned unbonded beams. *IOP Conf Ser Mater Sci Eng* 1030(1):012077. <https://doi.org/10.1002/suco.202000774>
11. Khatib M, Abou Saleh Z, Baalbaki O, Hamdan Z (2022) Numerical shear of post-tensioned beams with inverted-U shaped reinforcements. *Mag Civil Eng* 110(2). <https://doi.org/10.34910/MCE.110.6>
12. ACI Committee 318 (2011) Building code requirements for structural concrete (ACI 318–11) and Commentary. American Concrete Institute, Farmington Hills, 503 pp
13. Freyeremuth CL (1989) Structural integrity of buildings constructed with unbonded tendons. *Concr Int* 11(3):56–63
14. ABAQUS, 6.13 (2013) ABAQUS/CAE user's guide, Providence
15. Rogers J (2006) PT concrete in the residential industry. *Concrete Constr Mag*
16. Bondy KB (2012) Two-way PT slabs with bonded tendons. *PTI J* 8(2):43–48
17. Lubliner J, Oliver J, Oller S, Oñate E (1989) A plastic-damage model for concrete. *Int J Solids Struct* 25:229–326
18. Lee J, Fenves GL (1998) Plastic-damage model for cyclic loading of concrete structures. *J Eng Mech* 124:892–900
19. Carreira DJ, Chu KH (1985) Stress-strain relationship for plain concrete in compression. *ACI J Proc* 83(6):797–804
20. Hamoda A, Basha A, Fayed S et al (2019) Experimental and numerical assessment of reinforced concrete beams with disturbed depth. *Int J Concrete Struct Mater* 13(55). <https://doi.org/10.1186/s40069-019-0369-5>.
21. Seok S, Haikal G, Ramirez JA, Lowes LN, Lim J (2020) Finite element simulation of bond-zone behavior of pullout test of reinforcement embedded in concrete using concrete damage-plasticity model 2 (CDPM2). *Eng Struct* 221(15). <https://doi.org/10.1016/j.engstruct.2020.110984>
22. Liu J, Shi C, Lei M, Wang Z, Cao C, Lin Y (2022) A study on damage mechanism modelling of shield tunnel under unloading based on damage–plasticity model of concrete. *Eng Fail Anal* 123. <https://doi.org/10.1016/j.engfailanal.2021.105261>
23. Kang TH-K, Huang Y (2012) Nonlinear finite element analyses of unbonded post-tensioned slab-column connections. *PTI J* 8(1):4–19
24. Devalapura RK, Tadros MK (1992) Critical assessment of ACI 318 Eq. (18–3) for prestressing steel stress at ultimate flexure. *ACI Struct J* 89(5):538–546

Open Access This chapter is licensed under the terms of the Creative Commons Attribution 4.0 International License (<http://creativecommons.org/licenses/by/4.0/>), which permits use, sharing, adaptation, distribution and reproduction in any medium or format, as long as you give appropriate credit to the original author(s) and the source, provide a link to the Creative Commons license and indicate if changes were made.

The images or other third party material in this chapter are included in the chapter's Creative Commons license, unless indicated otherwise in a credit line to the material. If material is not included in the chapter's Creative Commons license and your intended use is not permitted by statutory regulation or exceeds the permitted use, you will need to obtain permission directly from the copyright holder.

